Sensors and Actuators A 303 (2020) 111863

Contents lists available at ScienceDirect

Sensors and Actuators A: Physical

journal homepage: www.elsevier.com/locate/sna

# Characterization of a parametric resonance based capacitive ultrasonic transducer in air for acoustic power transfer and sensing

Sushruta Surappa, F. Levent Degertekin*

*Woodruff School of Mechanical Engineering, Georgia Institute of Technology, Atlanta, GA 30313, USA*

ARTICLE INFO

*Article history:*
Received 28 October 2019
Received in revised form 13 January 2020
Accepted 22 January 2020
Available online 24 January 2020

*Keywords:*
Parametric resonance
Airborne ultrasound
Capacitive parametric ultrasonic transducer
Acoustic power transfer
Sensing
Highly directional acoustic sensor

ABSTRACT

Capacitive transducers typically require a DC bias or a pre-charged electret to operate, rendering them non-ideal for applications such as energy harvesting and wireless power transfer. Parametric resonance based capacitive transducers offer an alternative to traditional capacitive transducers as they can be operated without the need for a bias voltage or a pre-charged electret. In this paper, we experimentally validate a 1D lumped parameter model and characterize a CPUT operating in air at 50 kHz for ultrasonic power transfer and sensing applications. This particular CPUT is able to recover 40.5 μW of power at an efficiency of 0.32% without any DC bias when excited by a 50 kHz piezoelectric transducer. The application of the CPUT as a highly sensitive acoustic sensor is explored by making use of active electrical circuits that reduce the resistance of the system. Finally, the capability of the CPUT as a highly directional acoustic sensor is presented with the electrostatic transducer demonstrating a directivity of $\pm 1^\circ$ when operated as a CPUT as compared to $\pm 13^\circ$ when operated as a conventional biased receiver. These results set the stage for the application of CPUT as a multi-functional acoustic transducer.



## 1. Introduction

Capacitive transducers have long been used for a variety of applications such as sensing [1–3], medical imaging [4–6], energy harvesting [7–9] and for wireless power transfer [10,11]. Compared to their piezoelectric counterparts, capacitive transducers can be easily realized in various geometries and sizes thanks to advances in silicon micromachining processes. Furthermore, the operating frequency of capacitive transducers is not limited by the size of the transducer as is the case with piezoelectric crystals. The advantage of miniaturization, large bandwidth and ease of electronics integration [12] make capacitive transducers highly desirable for various applications.

Despite these benefits, a DC voltage or a bias must be provided to a capacitive transducer in order to ensure it operates efficiently. This places a significant limitation on them as they cannot be used for applications where the supply of a large bias voltage is impractical or dangerous. Although pre-charged or electret-based devices have been explored to circumvent this drawback [13], piezoelectric transducers are preferred for applications such as energy harvesting or wireless power transfer as they do not require any bias voltage for operation. Recently we reported a new type of acoustic capacitive transducer that can work in the absence of a DC bias or pre-charge, called the capacitive parametric ultrasonic transducer (CPUT) [14]. The CPUT consists of a time varying, membrane-based capacitor connected in series with an inductor and resistor to form a series RLC circuit. An ultrasonic wave incident on the membrane is used to drive the RLC circuit into parametric resonance (PR), thereby converting the acoustic energy to an electrical signal.

Parametric resonance is a phenomenon in which an electrical or mechanical system can be driven into oscillations of large amplitude by varying some internal parameter of the system. Unlike direct resonance, in which a force is applied on a system at its natural frequency, primary PR is commonly obtained by varying a system parameter such as the stiffness (for mechanical systems) or capacitance (for electrical systems) around two times the natural frequency. PR-based devices have been in use since the mid 1900's and first found prominence as low noise electrical amplifiers [15,16]. Advances in micromachining techniques led to the development of various PR based MEMS transducers used for applications such as force and mass sensing [17–23], angular rate sensing [24,25], as tunable filters [26] and amplifiers [27]. More recently, energy harvesting systems have made use of PR as a means of mechanical pre-amplification to increase the efficiency and bandwidth of vibration energy harvesters [28–31]. However, despite the various attractive features of using PR-based devices for sensing

* Corresponding author.
*E-mail address:* levent.degertekin@me.gatech.edu (F.L. Degertekin).

https://doi.org/10.1016/j.sna.2020.111863

and energy harvesting, the technique has certain limitations holding it back from widespread adoption. Firstly, a damping dependant initiation threshold must be overcome to drive the system into PR [32]. This condition requires that large forces be applied to drive mechanical systems into parametric resonance due to the damping and losses in the environment. Although this requirement can be partially overcome by clever design of systems [30,33], current PR-based mechanical systems are unsuitable for operation in lossy environments. Secondly, PR is used mainly as a means of mechanical pre-amplification and a second transducer (usually electrical or optical) is usually employed to convert the input signal into an electrical readout. Naturally, this two-stage implementation increases the size and complexity of the system. Both of the above mentioned drawbacks are addressed by the CPUT, as the input ultrasonic energy is directly converted to a readable electrical output without the requirement of a secondary transducer. Furthermore, the initiation threshold for PR is strongly dependent on the electrical resistance of the CPUT. This feature enables the operation of the CPUT even in lossy environments as it is easier to control the electrical resistance of the device as compared to the mechanical damping due to the surrounding fluid. The absence of bias voltage, single-step transduction and tunable initiation threshold, makes the CPUT a highly versatile PR-based capacitive transducer.

Previously, simulations performed using a 1D lumped parameter model suggested that the CPUT could be used for acoustic power transfer in water and air [34]. In this paper, we validate the 1D model and explore the operational characteristics of a CPUT operating in air excited by a 50 kHz ultrasonic source. Performance parameters such as output power and efficiency are experimentally evaluated as a function of input pressure, forcing frequency and load resistance - these results are compared with simulations to confirm the validity of the 1D lumped parameter model and demonstrate the merits of the CPUT as a bias-free receiver for acoustic power transfer. We also take advantage of two characteristics which are unique to the CPUT – an adjustable initiation threshold and an asymmetric frequency response, to demonstrate the advantages of the CPUT over other parametrically driven systems for acoustic sensing applications.

## 2. Theory

A brief review of parametric resonance is presented in this section, followed by the principle of operation of the CPUT for the sake of completeness. While a simple system undergoing linear parametric resonance can be represented by the Mathieu's equation, the CPUT is a complex system comprising of a coupled electrical and mechanical resonator. The 1D lumped parameter model that is used to describe the operation of the CPUT is briefly described along with two separate methods of solution for the model.

### 2.1. Parametric resonance in CPUT

Parametric resonance is obtained when some internal parameter of a system is periodically varied at a frequency that is an integer or a fractional multiple of the resonance frequency of the system. The behavior of such systems can be represented by the Mathieu's equation:

$$\frac{d^2u}{dt^2} + (a + Bcos(\Omega t))u = 0 \tag{1}$$

where the term $Bcos(\Omega t)$ acts an energy/pump source and is said to parametrically excite the system. Principle PR is obtained when $\Omega$ is around two times the natural frequency of the system, and an unstable, exponentially growing solution to the equation is obtained. Unlike in direct resonance, the presence of damping does not limit the response of the parametrically excited system.

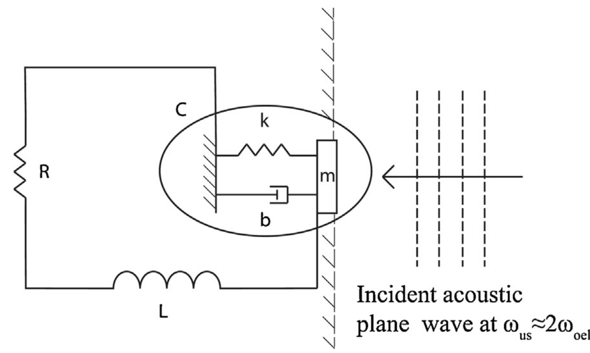


**Fig. 1.** 1D lumped parameter model of CPUT.

However, a higher level of damping will require a greater pump amplitude $B$ to exceed an initiation threshold and drive the system into PR. While Mathieu's equation represents a purely linear parametric resonator with an unbounded solution, real-world systems respond with some degree of nonlinearity, which eventually limits the magnitude of response of the parametrically excited system.

The CPUT is one such system, comprised of a time-varying capacitor connected in series with an inductor and a resistor to form a series RLC circuit having a resonance frequency $f_0$. The time-varying capacitor can be a membrane-based mechanical device such as an electrostatic transducer or a capacitive micromachined ultrasonic transducer. The capacitance of the RLC circuit is modulated by exciting the mechanical membrane using ultrasonic waves of frequency $2f_0$ (pump source). When the capacitance modulation exceeds the initiation threshold, the RLC circuit is pumped into PR and the incident acoustic energy is converted to electrical energy. Unlike direct resonance, some initial oscillation must be present in the electrical circuit in order to drive it into PR. This condition can be satisfied by the thermomechanical noise present in the system, although in the experiments reported in this paper, it is satisfied by the electromagnetic coupling between the ultrasonic source and the CPUT, making it a self-starting device.

#### 2.1.1. 1D lumped parameter model

The CPUT can be represented by a 1D lumped parameter model as shown in Fig. 1. In this model, the membrane-based receiver is modelled as a parallel plate piston of known mass $m$, stiffness $k$ and damping $b$. The values of $m$, $k$ and $b$ are extracted from the dynamics of the actual capacitive transducer used in the experiments and it is assumed that the motion of the piston is uniform. The piston behaves as a variable capacitor in the electrical domain and is connected to an inductor $L$ and a resistor $R$ to complete the RLC circuit. The incident ultrasonic field is simulated by applying a uniform force on the face of the piston. The 1D lumped parameter model can be expressed mathematically in the form of two coupled ordinary differential equations (ODE) as:

$$\left[\frac{d^2}{dt^2} + \frac{R}{L}\frac{d}{dt} + \frac{d_0 - x}{LA\varepsilon_0}\right] V = 0 \tag{2}$$

$$\left[\frac{d^2}{dt^2} + \frac{b}{m}\frac{d}{dt} + \frac{k}{m}\right] x = \frac{F_0}{m}\sin(\omega_{us}t) + \frac{\varepsilon_0 A}{2m}\frac{V^2}{(d_0 - x)^2} \tag{3}$$

where $d_0$, $x$, $A$, $V$, $F_0$ and $\omega_{us}$ represent the initial gap between the plates, displacement of plate, area of plate, voltage across capacitor, amplitude of ultrasonic forcing and frequency of ultrasonic forcing respectively. When the frequency of the incident ultrasonic excitation ($\omega_{us}$) is approximately twice the resonance frequency of the RLC circuit ($\omega_{oel} = \frac{1}{\sqrt{LC}}$), the system is driven into PR and a voltage develops across the capacitor which settles to a steady value determined by the nonlinearities in the system. Thus the 1D model can be used to predict the performance of the CPUT as a function of various parameters such as input forcing, excitation frequency, load resistance, etc. The solutions to the model are obtained by either simulating the electromechanical circuit in Simulink or by making use of approximate analytical solutions based on averaging methods as described in [35]. A more detailed treatment of the lumped parameter model and methods of solution is presented in [34].

## 3. Experimental setup

In order to validate the 1D lumped parameter model and characterize the CPUT, experiments are performed on a device operating in air. A schematic of the experimental setup is shown in Fig. 2a. A commercially available 50 kHz electrostatic transducer (500ES430, Prowave inc, Taiwan) is connected in series with a 128 mH inductor and a resistance box to form the CPUT. The unbiased, static capacitance of the electrostatic transducer and the resonance frequency of the RLC circuit is measured using a network analyzer (Agilent 8753ES) and is found to be 340 pF and 24.22 kHz respectively. The electrostatic transducer is mounted on a 20 cm × 20 cm wooden baffle in order to mimic the baffled piston condition used in the simulations. Note that while the recommended bias voltage for the electrostatic transducer is 200 VDC, no bias voltage is supplied in the current configuration. An oscilloscope (Tektronix TDS 5054) is used to measure the voltage across the resistance box for different values of load resistance. A 50 kHz piezoelectric transducer (Prowave inc, 500MB120) is used as the ultrasonic source and is placed 7 cm away from the electrostatic receiver. A signal generator (Agilent 33250A) connected to an amplifier with a gain of 20× (EPA-104, Piezo Systems inc.) is used to drive the piezoelectric transmitter.

A calibrated measurement microphone (Larson and Davis model 2520) is used to characterize the acoustic pressure incident on the CPUT receiver. Since the acoustic wavelength is smaller than the size of the receiver, the incident pressure field is non-uniform. A 6 cm by 6 cm square grid is scanned (Fig. 2c) and the pressure recorded at each point is summed and averaged to obtain an average RMS acoustic pressure $p$ on the face of the receiver. The available power is then defined as $\frac{p^2}{2\rho c}$, where $\rho$ is the density of air and $c$ is the speed of sound in air. Based on this, the acousto-electrical efficiency of the CPUT is defined as:

$$Efficiency = \frac{\frac{1}{T}\int_0^T i^2 R dt}{Available \quad power} \times 100(\%) \tag{4}$$

where $i$ is the amplitude of current in the RLC circuit. The efficiency of the CPUT is then calculated for different input forcing, frequency and resistive loading conditions.

## 4. Results and discussion

The simulation tools developed in Section 2 along with the experimental setup described in Section 3 enables the investigation of the various operational characteristics of the CPUT. In this section, we benchmark the performance of the CPUT for acoustic power transfer and sensing to validate the 1D lumped parameter model and to demonstrate the versatility of the CPUT as an acousto-electrical transducer.

### 4.1. Acoustic power transfer

Various technological advances in consumer electronics, wearables and Internet of Things (IoT) has rekindled interest in ultrasonic wireless power transmission through air [10,36–39]. The ability to operate the CPUT without a bias voltage makes it a prime candidate to function as a receiver for such applications. Previously, simulations indicated that the CPUT could function as a highly efficient receiver for ultrasonic power transfer in water [34]. The power transfer performance of the CPUT in air is simulated using the 1D model and compared with experimental results in this section.

**Table 1**
Parameters used for simulations.

| Symbol | Parameter | Value |
|---|---|---|
| $\rho$ | Fluid density | 1.21 kg/m$^3$ |
| $c$ | Speed of sound | 340 m/s |
| $m$ | Piston mass | $1.072 \times 10^{-7}$ kg |
| $k$ | Piston stiffness | $1 \times 10^4$ N-m |
| $b$ | Piston damping | 1.13 kg/s |
| $A$ | Piston area | 0.0011 m$^2$ |
| $d_0$ | Vacuum gap | 10 μm |

#### 4.1.1. Simulation results

The parameters used in the simulation of a CPUT operating in air are listed in Table 1. The main challenge in obtaining the simulation parameters is that the electrostatic transducer (500ES430, Prowave inc, Taiwan) used in the experiments operates differently from the simplistic parallel plate model used in the simulation. The Prowave transducer makes use of a polymer membrane stretched across a grooved backplate, similar to the capacitive transducer reported in [40]. Due to the unavailability of an operational model for such a design in literature, the lumped parameters for the transducer are chosen such that the simulations fit the frequency bandwidth data obtained from the CPUT experiments. This choice of parameters is justified as the simulation results are also consistent with other experimental data as shown later in Section 4.1.2.

The average pressure measured on the face of the CPUT using the measurement microphone is applied as the forcing excitation in the simulations. The power dissipated across the load resistance for three different input intensities at 48.6 kHz is plotted in Fig. 3a. It is observed that the dissipated power increases to a maximum value before reducing to zero as the resistance is increased. The resistance at which maximum power is obtained corresponds to the best impedance match between the CPUT and the electrical load. Further increasing the resistance causes a gradual decline in output power until it reaches zero. At this value of resistance, the forcing threshold required for PR is above the input forcing level, thereby preventing the CPUT from being driven into PR. Further increasing the input forcing enables the CPUT to be operated over a larger range of load resistance, however, the nonlinear nature of the device causes a shift in the optimal load resistance. Hence, prior knowledge of the range of input forcing helps in the selection of an optimal value of load resistance for power transfer.

The frequency response of the CPUT is simulated by recording the maximum steady state voltage across a load resistance of 100 Ω while linearly sweeping though the forcing frequency. The operational bandwidth of the CPUT for different levels of input forcing is shown in Fig. 3b. It can be seen that the voltage across the resistor is negligible at the start of the frequency sweep and this corresponds to a region of no PR. As the frequency is increased to approximately twice the resonant frequency of the RLC circuit, the system transitions from a region of no PR to a region of PR and this transition is accompanied by a sharp increase in resistor voltage. As the frequency is increased further, the voltage gradually decreases until it once again becomes negligible and the system is detuned from PR. This region in which the CPUT is driven into PR is typically known as an instability tongue and has been previously derived for an ideal CPUT without parasitics using Eqs. (2) and (3) in [34]. Increasing the input forcing leads to the broadening of the instability tongue accompanied by a larger peak response thereby increasing the output voltage and operational bandwidth of the CPUT. The nonlinearities present in the parametrically excited system cause the

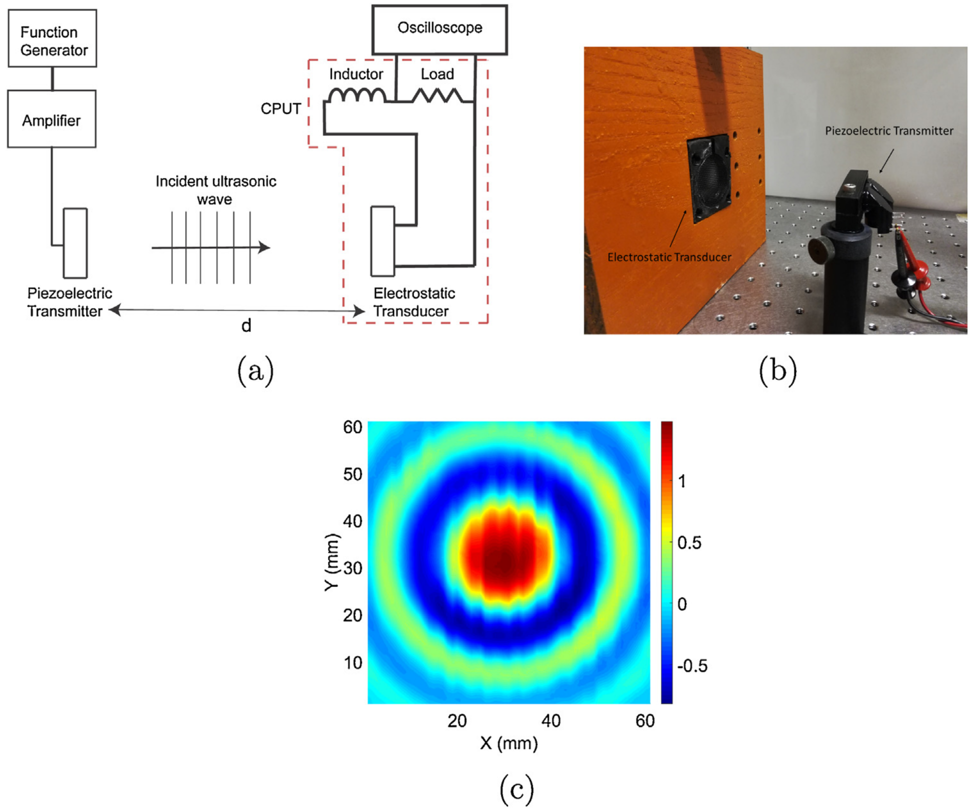


**Fig. 2.** (a) Schematic of the experimental setup (b) Actual experimental setup (c) Source pressure distribution as recorded by a measurement microphone.

instability tongue to display an asymmetric frequency response, which is responsible for the sharp increase in resistor voltage as the CPUT transitions into PR at its lower frequency boundary. This transition occurs over a very narrow frequency band and finds application in sensing, which will be discussed in greater detail in Section 4.1.2.

The most important metric in power transfer applications is the acousto-electric efficiency of the transducer. The CPUT efficiency is expressed as a 2D color map, with forcing frequency on the *y*-axis and the input power on the *x*-axis (Fig. 3c). The range of frequencies in which the CPUT is driven into PR increases with increased forcing as explained previously. Due to the asymmetric nature of the frequency response, the regions of maximum efficiency tend towards a lower frequency and increase with greater available power. Although simulations indicate that the maximum achievable efficiency is less that 1%, it must be noted that power transfer is achieved in the absence of a large bias voltage. Furthermore, a significant increase in efficiency can be obtained by reducing the compliance of the membrane and decreasing the squeeze film losses in the air gap of the electrostatic transducer. It is found that increasing the stiffness of the membrane by a factor of 5 while keeping all of the other simulation parameters the same leads to a 4× increase in CPUT efficiency.

### 4.1.2. Experimental results

The primary aim of the experiments is to demonstrate the feasibility of acoustic power transfer using the CPUT and to validate the simulation results presented in Section 4.1.1. The results obtained for power transfer in air closely follow the trends observed in the simulation results and are presented in Fig. 4. A maximum power of 2 μW, 13.7 μW and 20.5 μW is dissipated across a load resistance of 50 Ω, 140 Ω and 160 Ω respectively for three increasing input intensities (Fig. 4a). In comparison, the maximum power obtained in the simulations for the same input intensities are 2.95 μW, 6.4 μW and 11 μW, with the discrepancy between simulation and experiment increasing with increased forcing. The simulations only slightly under-predict the maximum allowable load resistance for the three increasing input intensities (160 Ω, 240 Ω and 300 Ω from simulations vs. 170 Ω, 280 Ω and 360 Ω from experiment) and this can be attributed to errors in estimation of the parasitic capacitance and damping parameters used in the simulation. For similar reasons, the experimental frequency bandwidth (Fig. 4b) is greater than that predicted by the simulation by 62% for an input intensity of 5.85 W/m$^2$ and the difference increases to 78% for an intensity of 11.6 W/m$^2$. The output voltage for an intensity of 11.6 W/m$^2$ sharply increases from 0 V at 47.78 kHz to 90 mV at 47.84 kHz before gently decreasing to 0 V at 49.34 kHz. The peak voltage corresponds to an average power of 40.5 μW obtained across a load resistance of 100 Ω without a DC bias. The efficiency map in Fig. 4c indicates that a peak efficiency of 0.32% for an input acoustic intensity of 11.6 W/m$^2$ closely matches the predicted efficiency of 0.35% by the simulation. However, the experimental results indicate a drop in peak efficiency down to 0.11% as the input forcing is reduced to 5.85 W/m$^2$ whereas the peak efficiency stays approximately constant in the simulation.

Overall, these results indicate that the simple 1D model is valid for predicting the performance and trends of a CPUT operating in air. Note that the commercial electrostatic transducer used in the experiments has large parasitic capacitance and damping that negatively affects the power transfer performance of the CPUT. We have previously shown that increasing the mechanical Q-factor of the receiver by the use of less compliant membranes leads to a higher power transfer efficiency [34]. Improving the receiver design by vacuum sealing the gap [41] and making use of a mass loaded membrane [42] enables one to obtain a large mechanical Q-factor in any medium of operation. Similarly, parasitic capacitance can be minimised by reducing the electrode coverage over non-active

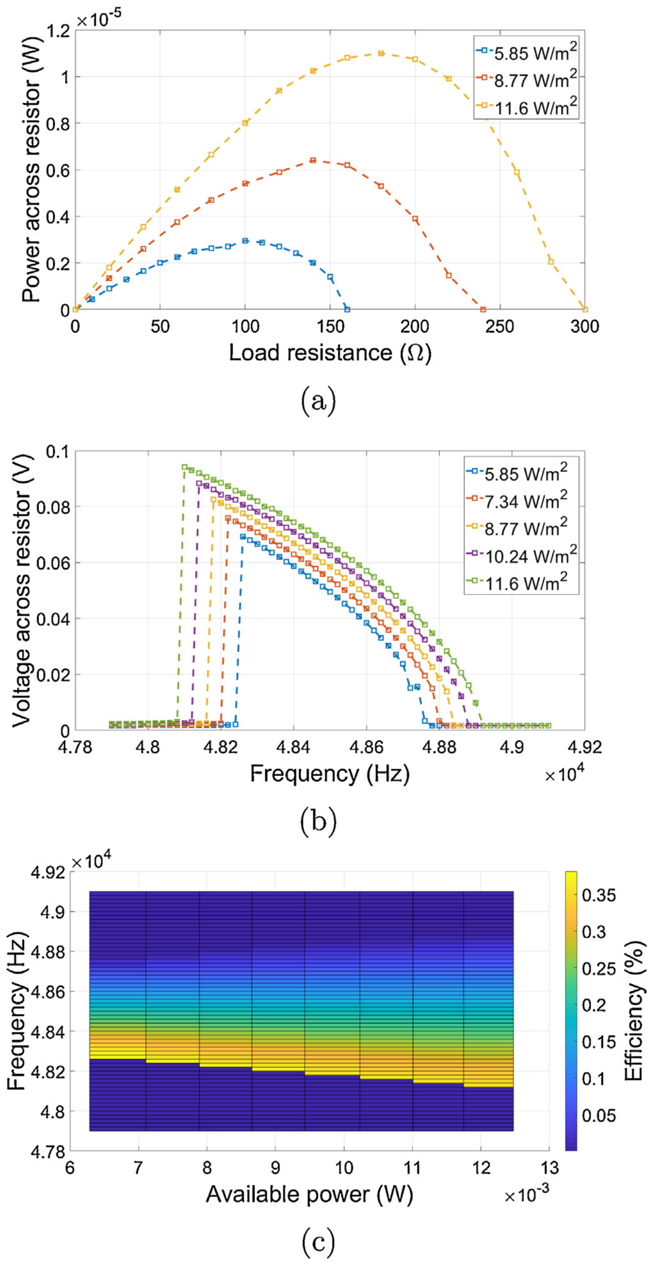


**Fig. 3.** Simulations performed using the 1D model yield (a) Power measured across load vs. load resistance for different values of input forcing at 48.6 kHz. (b) The operational bandwidth of the CPUT as a function of input forcing. (c) Efficiency of the CPUT as a function of input forcing level and frequency.

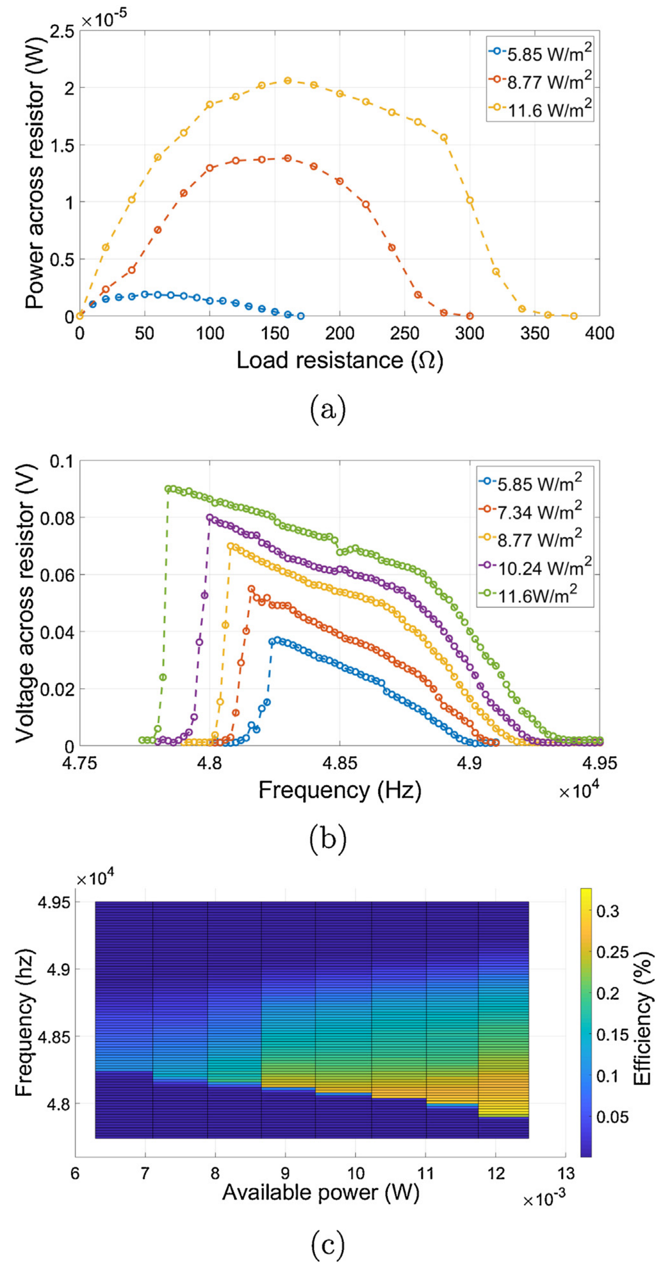


**Fig. 4.** Experimental results for power transfer in air (a) Power measured across load vs. load resistance for different values of input forcing at 48.6 kHz. (b) The operational bandwidth of the CPUT as a function of input forcing. (c) Efficiency of the CPUT as a function of input forcing level and frequency.

areas of the transducer and making use of improved microfabrication techniques such as the oxide lift-off [43].

#### 4.1.3. *Tunable initiation threshold*

Unlike resonant sensors, the response amplitude of a system driven into PR is not limited by the damping present in the environment. However, damping directly affect the initiation threshold required for PR in mechanical systems operating in lossy environments such as water and blood, as larger damping requires a greater force to drive the system into PR. The CPUT has a distinct advantage when compared to mechanical PR based systems as the losses in an electrical circuit can be easily reduced by making use of active circuits that behave as a negative resistance. While acoustic power transfer requires the CPUT to be a completely passive device, sensing applications do not place the same restrictions on the use of active circuits. Using such circuits, the losses in the RLC circuit can be minimized, thus enabling the detection of a very small acoustic pressure.

As an example, one such implementation of an active circuit in the CPUT is shown in Fig. 5a. In order to reduce the losses in the RLC circuit, a tunable, op-amp based negative resistance circuit [44] is connected in parallel with the inductor. The value of the negative resistance can be chosen such that it partly or wholly cancels the internal resistance of the RLC circuit. In order to demonstrate that the forcing threshold to drive the CPUT into PR can be dramatically lowered, the voltage across the capacitor is plotted as a function of the input voltage to the piezoelectric transmitter for two cases (Fig. 5b). In the first case, no active circuitry is used, and the capacitor voltage is measured for a zero load resistance condition. It is seen that a minimum voltage of 36 V must be applied to the transmitter

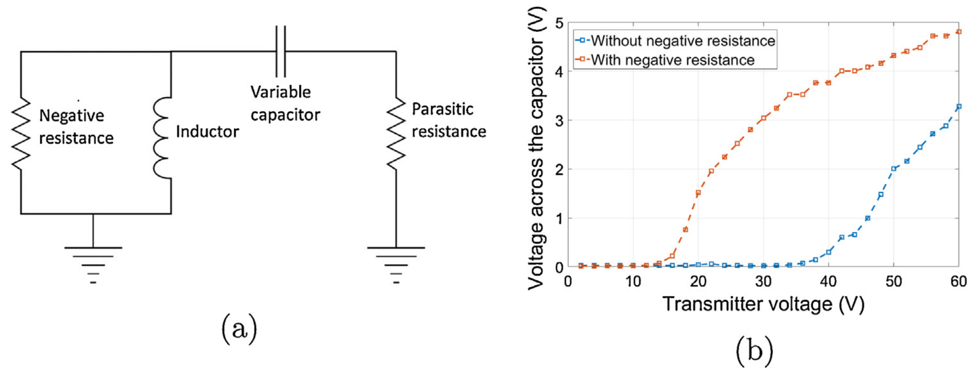


**Fig. 5.** (a) Implementation of negative resistance in RLC circuit. (b) Impact of negative resistance in lowering the forcing threshold for PR in CPUT.

to drive the CPUT into PR due to the internal resistance present in the system. In the second case, a portion of the internal resistance is cancelled using an equivalent negative resistance of −160 Ω and in this case the system requires only 14 V to be driven into PR. Further reducing the losses with a greater value of negative resistance can lead to a lower threshold for PR and higher sensitivity. In contrast, PR driven mechanical systems must be operated in high vacuum conditions in order to lower initiation threshold, thereby limiting their application in different environments. In addition the CPUT directly converts the input force into a measurable voltage thereby circumventing the need for a secondary detection transducer hence reducing the size and complexity of the system. However, one must consider the fact that the active circuit injects noise into the system, and the ultimate sensitivity of the CPUT is eventually limited by the thermomechanical noise [17,45]. Besides, sensing applications, the ability to control the initiation threshold will also find applications in PR based energy harvesters, where complex mechanical designs are currently used to reduce the force required for PR [30,29].

#### 4.1.4. Exploiting the asymmetric frequency response for highly directional acoustic receiver

Parametrically excited systems are known to display an asymmetric frequency response due to nonlinearties present in the system [46]. In the case of the CPUT, the $V^2$ term in the right hand side of Eq. (3) results in a net attractive force on the membrane of the capacitor, which in turn increases the average capacitance. This softening nonlinearity leads to a left leaning asymmetric instability tongue as seen in Fig. 3b. When the system is operated at the leading edge on the left, a small reduction in the forcing amplitude or frequency causes the system to transition out of the instability tongue where PR cannot be sustained, hence leading to a sharp drop in response amplitude.

We exploit this asymmetric frequency response to demonstrate that the CPUT can be used as an acoustic receiver with an adjustable directivity. The experimental setup described in Section 3 is used to measure the directivity of the electrostatic transducer by mounting it on a rotational stage. First, a DC bias of 50 V is applied across the terminals of the transducer and the output AC voltage is measured for different angles of incidence when excited by a tone burst from the piezoelectric transmitter. The bias voltage is then removed and the electrostatic transducer is connected to an inductor and resistor to form a CPUT. The output AC voltage is once again measured for different incidence angles when the transmitter forcing frequency is approximately twice the RLC resonant frequency. The results shown in Fig. 6 indicate a good match between the experimentally measured directivity when biased and the analytical solution for the directivity of a baffled circular piston. According to the analytical solution, the main lobe should approximately lie between +13° and −13° and the experimental deviation could be a result of

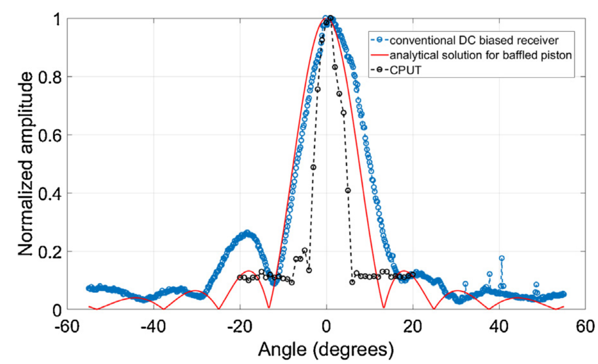


**Fig. 6.** Directivity of receiver measured while operating device in conventional DC biased mode and as CPUT.

imperfect alignment between the source and receiver. In contrast, the main lobe only spans from −5° to +5° when operated as a CPUT. The narrower beam width is also accompanied by a lack of side-lobes, as the CPUT is only sensitive to acoustic pressure levels that exceeds the threshold required for PR. As the angle of incidence exceeds ±5°, the average pressure on the face of the transducer drops below the level required to sustain PR, effectively causing the CPUT to become insensitive to the incident acoustic field.

The directivity beam width of the CPUT is determined by the excitation amplitude and the frequency of the incident acoustic wave. Fig. 7a shows the experimentally measured beam width in parametric mode as a function of the forcing amplitude where it can be seen that the beam width increases as the forcing is increased. This can be explained by referring to Fig. 3b where it can be seen that increasing the forcing leads to a broadening of the instability tongue. Hence for a fixed frequency, a larger input force allows for a greater angle of incidence before the average pressure on the face of the CPUT falls below the threshold required for PR. Similarly, it can be seen in Fig. 7b that a very narrow beam spanning approximately ±1° can be achieved when the incident frequency is 48.4 kHz. This frequency corresponds to a point at the leftmost edge of the asymmetric instability tongue where even a small change in incidence angle reduces the average pressure, which in turn causes the narrowing of the tongue and detunes the CPUT from PR. When the frequency is increased to 48.5 kHz, the CPUT is now operated in the middle of its instability tongue, and is therefore less sensitive to small changes in incident pressure, allowing the CPUT to be sensitive over a larger range of incidence angles. Note that the output voltage amplitude of the CPUT has been normalized with respect to itself in both Figs. 7a and b. It is important to mention that the excitation amplitude can be controlled internally by making use of a drive mechanism such as one described in [47,48] whereas the PR frequency band of the CPUT can be shifted by active tuning of

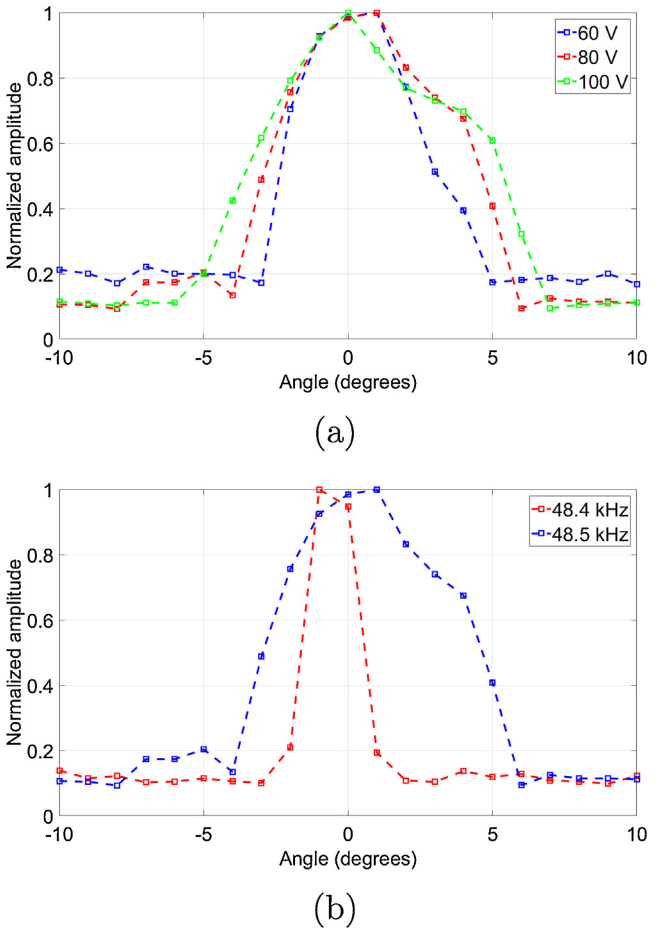


**Fig. 7.** CPUT directivity as a function of (a) input excitation amplitude and (b) input excitation frequency.

circuit parameters. Hence it is possible to internally adjust both the excitation amplitude and CPUT operating frequency to ensure a high degree of directivity is obtained independent of the amplitude and frequency of the incident acoustic wave. Such a system can potentially be employed to increase the directivity of a nearly omnidirectional receiver which has physical dimensions smaller than the incident acoustic wavelength [49].

## 5. Conclusion

In this work, we experimentally validate a 1D lumped parameter model and characterize a CPUT for acoustic power transfer and sensing applications by making use of a commercially available electrostatic air transducer. The power transfer efficiency of the CPUT is experimentally evaluated as a function of load resistance, input acoustic intensity and forcing frequency. It is found that a peak output power of 40.5 $\mu$W is obtained across a load resistance of 100 $\Omega$ at an efficiency of 0.32% without the need for a bias voltage or precharged electret. This efficiency, which is in agreement with simulation results, can be further improved by making use of a stiffer membrane and reducing the losses associated with parasitic capacitance and squeeze film damping in the electrostatic transducer. We further demonstrate that the threshold required for PR can be dramatically reduced by making use of active electrical circuits. In contrast with purely mechanical PR based systems, the electrical resistance of the CPUT can be reduced to make it extremely sensitive to acoustic signals even in a damped environment such as water thereby presenting opportunities in acoustic sensing. Finally, we discuss the feasibility of operating the CPUT as an acoustic sensor with adjustable directivity by taking advantage of its asymmetric frequency response. It is observed that an acoustic directivity of $\pm 1^{\circ}$ can be obtained by operating this particular CPUT at the edge of its instability tongue as compared to a directivity of $\pm 13^{\circ}$ when operated with a DC bias as a conventional capacitive sensor.

This study indicates significant potential for the operation of a CPUT as an acoustic transducer. The nonlinear device characteristics and direct energy conversion capability facilitates the use of a CPUT for acoustic power transfer and sensing. Future work includes the design and optimization of CPUTs.

## Author contributions

**Sushruta Surappa**: Concept development and analysis, experiment design and implementation, data interpretation, writing of manuscript.

**F. Levent Degertekin**: Concept development and analysis, experiment design and implementation, data interpretation, writing of manuscript.

## Conflicts of interest

The authors declare no conflicts of interest.

## Acknowledgements

This work was supported by the ECCS Division of the National Science Foundation through NSF ECCS under Award 1936776 and 1829821.

## References

[1] P.R. Scheeper, A.G.H. Van der Donk, W. Olthuis, P. Bergveld, A review of silicon microphones, Sens. Actuators A: Phys. 44 (1994) 1–11.
[2] A. Torkkeli, O. Rusanen, J. Saarilahti, H. Seppä, H. Sipola, J. Hietanen, Capacitive microphone with low-stress polysilicon membrane and high-stress polysilicon backplate, Sens. Actuators A: Phys. 85 (2000) 116–123.
[3] C. Seok, M.M. Mahmud, M. Kumar, O.J. Adelegan, F.Y. Yamaner, M. Oralkan, A low-power wireless multichannel gas sensing system based on a capacitive micromachined ultrasonic transducer (CMUT) array, IEEE Internet Things J. 6 (2018) 831–843.
[4] T. Xu, C. Tekes, F. Degertekin, CMUTs with high-K atomic layer deposition dielectric material insulation layer, IEEE Trans. Ultrason. Ferroelectr. Freq. Control 61 (2014) 2121–2131.
[5] F.L. Degertekin, R.O. Guldiken, M. Karaman, Annular-ring CMUT arrays for forward-looking IVUS: transducer characterization and imaging, IEEE Trans. Ultrason. Ferroelectr. Freq. Control 53 (2006) 474–482.
[6] B.T. Khuri-Yakub, M. Oralkan, Capacitive micromachined ultrasonic transducers for medical imaging and therapy, J. Micromech. Microeng. 21 (2011) 054004.
[7] U. Bartsch, J. Gaspar, O. Paul, A 2d electret-based resonant micro energy harvester, IEEE 22nd International Conference on Micro Electro Mechanical Systems, 2009 (2009) 1043–1046.
[8] B.C. Yen, J.H. Lang, A variable-capacitance vibration-to-electric energy harvester, IEEE Trans. Circuits Syst. I: Regular Papers 53 (2006) 288–295.
[9] F. Peano, T. Tambosso, Design and optimization of a MEMS electret-based capacitive energy scavenger, J. Microelectromech. Syst. 14 (2005) 429–435.
[10] A.S. Rekhi, B.T. Khuri-Yakub, A. Arbabian, Wireless Power, Transfer to millimeter-sized nodes using airborne ultrasound, IEEE Trans. Ultrason. Ferroelectr. Freq. Control (2017) 1.
[11] S. Banerji, W.L. Goh, J.H. Cheong, M. Je, CMUT ultrasonic power link front-end for wireless power transfer deep in body, 2013 IEEE MTT-S International Microwave Workshop Series on RF and Wireless Technologies for Biomedical and Healthcare Applications (IMWS-BIO) (2013) 1–3.
[12] M.S. Salim, M.F. Abd Malek, R.B.W. Heng, K.M. Juni, N. Sabri, Capacitive micromachined ultrasonic transducers: technology and application, J. Med. Ultrasound 20 (2012) 8–31.
[13] M.C. Ho, M. Kupnik, K.K. Park, B.T. Khuri-Yakub, Long-term measurement results of pre-charged CMUTs with zero external bias operation, IEEE International Ultrasonics Symposium (2012) 89–92.
[14] S. Surappa, S. Satir, F. Levent Degertekin, A capacitive ultrasonic transducer based on parametric resonance, Appl. Phys. Lett. 111 (2017) 043503.
[15] P. Tien, Parametric amplification and frequency mixing in propagating circuits, J. Appl. Phys. 29 (1958) 1347–1357.

[16] G.L. Matthaei, A Study of the Optimum Design of Wide-Band Parametric Amplifiers and Up-Converters, IRE Trans. Microw. Theory Tech. 9 (1961) 23–38.
[17] D. Rugar, P. Grütter, Mechanical parametric amplification and thermomechanical noise squeezing, Phys. Rev. Lett. 67 (1991) 699–702.
[18] W. Zhang, K.L. Turner, Application of parametric resonance amplification in a single-crystal silicon micro-oscillator based mass sensor, Sens. Actuators A: Phys. 122 (2005) 23–30.
[19] G. Prakash, A. Raman, J. Rhoads, R.G. Reifenberger, Parametric noise squeezing and parametric resonance of microcantilevers in air and liquid environments, Rev. Sci. Instrum. 83 (2012) 065109.
[20] Y. Linzon, B. Ilic, S. Lulinsky, S. Krylov, Efficient parametric excitation of silicon-on-insulator microcantilever beams by fringing electrostatic fields, J. Appl. Phys. 113 (2013) 163508.
[21] S. Krylov, Y. Gerson, T. Nachmias, U. Keren, Excitation of large-amplitude parametric resonance by the mechanical stiffness modulation of a microstructure, J. Micromech. Microeng. 20 (2009) 015041.
[22] M. Pallay, S. Towfighian, A parametric electrostatic resonator using repulsive force, Sens. Actuators A: Phys. 277 (2018) 134–141.
[23] M. Daeichin, M. Ozdogan, S. Towfighian, R. Miles, Dynamic response of a tunable MEMS accelerometer based on repulsive force, Sens. Actuators A: Phys. 289 (2019) 34–43.
[24] L.A. Oropeza-Ramos, C.B. Burgner, K.L. Turner, Robust micro-rate sensor actuated by parametric resonance, Sens. Actuators A: Phys. 152 (2009) 80–87.
[25] A. Sarrafan, S. Azimi, F. Golnaraghi, B. Bahreyni, A. Nonlinear, Rate microsensor utilising internal resonance, Sci. Rep. 9 (2019) 8648.
[26] J.F. Rhoads, S.W. Shaw, K.L. Turner, R. Baskaran, Tunable microelectromechanical filters that exploit parametric resonance, J. Vib. Acoust. 127 (2005) 423–430.
[27] J.P. Raskin, A.R. Brown, B. Khuri-Yakub, G.M. Rebeiz, A novel parametric-effect MEMS amplifier, J. Microelectromech. Syst. 9 (2000) 528–537.
[28] Y. Jia, A.A. Seshia, An auto-parametrically excited vibration energy harvester, Sens. Actuators A: Phys. 220 (2014) 69–75.
[29] Y. Jia, J. Yan, K. Soga, A.A. Seshia, Parametric resonance for vibration energy harvesting with design techniques to passively reduce the initiation threshold amplitude, Smart Mater. Struct. 23 (2014) 065011.
[30] W. Yang, S. Towfighian, A parametric resonator with low threshold excitation for vibration energy harvesting, J. Sound Vib. 446 (2019) 129–143.
[31] Y. Kuang, M. Zhu, Parametrically excited nonlinear magnetic rolling pendulum for broadband energy harvesting, Appl. Phys. Lett. 114 (2019) 203903.
[32] A.H. Nayfeh, D.T. Mook, Nonlinear Oscillations, John Wiley & Sons, 2008.
[33] Y. Jia, J. Yan, K. Soga, A.A. Seshia, Parametrically excited MEMS vibration energy harvesters with design approaches to overcome the initiation threshold amplitude, J. Micromech. Microeng. 23 (2013) 114007.
[34] S. Surappa, M. Tao, F.L. Degertekin, Analysis and design of capacitive parametric ultrasonic transducers for efficient ultrasonic power transfer based on a 1-D lumped model, IEEE Trans. Ultrason. Ferroelectr. Freq. Control 65 (2018) 2103–2112.
[35] M. Tao, Simply Improved Averaging for Coupled Oscillators and Weakly Nonlinear Waves, 2018 arXiv:1806.07947 [physics].
[36] M.G.L. Roes, M.A.M. Hendrix, J.L. Duarte, Contactless energy transfer through air by means of ultrasound, IECON 2011 – 37th Annual Conference of the IEEE Industrial Electronics Society (2011) 1238–1243.
[37] A.S. Rekhi, A. Arbabian, Ultrasonic wake-up with precharged transducers, IEEE J. Solid-State Circuits 54 (2019) 1475–1486.
[38] T. Zaid, S. Saat, N. Jamal, S.H. Husin, Y. Yusof, S. Nguang, A development of acoustic energy transfer system through air medium using push-pull power converter, WSEAS Trans. Power Syst. 11 (2016) 35–42.
[39] V.F.-G. Tseng, S.S. Bedair, N. Lazarus, Phased array focusing for acoustic wireless power transfer, IEEE Trans. Ultrason. Ferroelectr. Freq. Control 65 (2017) 39–49.
[40] D.W. Schindel, D.A. Hutchins, L. Zou, M. Sayer, The design and characterization of micromachined air-coupled capacitance transducers, IEEE Trans. Ultrason. Ferroelectr. Freq. Control 42 (1995) 42–50.
[41] I.O. Wygant, M. Kupnik, J.C. Windsor, W.M. Wright, M.S. Wochner, G.G. Yaralioglu, M.F. Hamilton, B.T. Khuri-Yakub, 50 kHz capacitive micromachined ultrasonic transducers for generation of highly directional sound with parametric arrays, IEEE Trans. Ultrason. Ferroelectr. Freq. Control 56 (2009) 193–203.
[42] N.A. Hall, R. Guldiken, J. McLean, F.L. Degertekin, Modeling and design of CMUTs using higher order vibration modes [capacitive micromachined ultrasonic transducers], IEEE Ultrasonics Symposium, 2004, vol. 1 (2004) 260–263.
[43] A. Pirouz, F.L. Degertekin, Low temperature CMUT fabrication process with dielectric lift-off membrane support for improved reliability, J. Micromech. Microeng. 28 (2018) 085006.
[44] J.G. Linvill, Transistor negative-impedance converters, Proc. IRE 41 (1953) 725–729.
[45] A.N. Cleland, Thermomechanical noise limits on parametric sensing with nanomechanical resonators, New J. Phys. 7 (2005) 235.
[46] J.F. Rhoads, S.W. Shaw, K.L. Turner, J. Moehlis, B.E. DeMartini, W. Zhang, Generalized parametric resonance in electrostatically actuated microelectromechanical oscillators, J. Sound Vib. 296 (2006) 797–829.
[47] R. Guldiken, J. Zahorian, F. Yamaner, F. Degertekin, Dual-electrode CMUT with non-uniform membranes for high electromechanical coupling coefficient and high bandwidth operation, IEEE Trans. Ultrason. Ferroelectr. Freq. Control 56 (2009) 1270–1276.
[48] R.O. Guldiken, J. McLean, F.L. Degertekin, CMUTS with dual electrode structure for improved transmit and receive performance, IEEE Trans. Ultrason. Ferroelectr. Freq. Control 53 (2006) 483–491.
[49] L.E. Kinsler, A.R. Frey, A.B. Coppens, J.V. Sanders, Fundamentals of Acoustics, 4th ed., Wiley-VCH, 1999.

## Biographies

Sushruta Surappa received the B.S. degree in mechanical engineering from Visvesvaraya Technological University, India, in 2012, and the M.S. degree in mechanical engineering from the Georgia Institute of Technology, Atlanta, GA, USA, in 2015, where he is currently pursuing the Ph.D. degree with the Woodruff School of Mechanical Engineering. His research interests include the study of parametric resonance in electromechanical transducers and their applications in ultrasonic power transfer, energy harvesting, microfluidics, metrology and other fields of engineering.

F. Levent Degertekin received the B.S. degree in 1989 from the Middle East Technical University, Turkey; the M.S. degree in 1991 from Bilkent University, Turkey; and the Ph.D. degree in 1997 from Stanford University, CA, all in electrical engineering. He worked at the E.L. Ginzton Laboratory of Stanford University first as a Visiting Scholar during the 1992-93 academic year and then as an Engineering Research Associate from 1997 to 2000. He currently holds the G.W. Woodruff Chair in Mechanical Systems, and is a Professor at the G.W. Woodruff School of Mechanical Engineering and the School of Electrical and Computer Engineering, Georgia Institute of Technology, GA. His research interests have been in micromachined acoustic and opto-acoustic devices, integrated systems for medical ultrasound imaging, bioanalytical instrumentation, and atomic force microscopy. He has authored over 50 U.S. patents and over 100 journal publications. Dr. Degertekin was an associate editor for the IEEE Sensors Journal and currently serves as an associate editor for the IEEE Transactions on Ultrasonics, Ferroelectrics and Frequency Control. Dr. Degertekin has received an NSF CAREER award for his work on ultrasonic atomic force microscopy in 2004, and with his students, the IEEE Ultrasonics, Ferroelectrics, and Frequency Control (UFFC) Society 2004 Outstanding Paper award, and most recently the IEEE UFFC Society 2014 Carl Hellmuth Hertz Ultrasonic Achievement Award.